AEM
Journals.ASM.org

Metabolic Engineering of *Escherichia coli* for the Synthesis of the Plant Polyphenol Pinosylvin

Philana Veronica van Summeren-Wesenhagen, Jan Marienhagen

Institute of Bio- and Geosciences, IBG-1: Biotechnology, Forschungszentrum Jülich GmbH, Jülich, Germany

Plant polyphenols are of great interest for drug discovery and drug development since many of these compounds have health-promoting activities as treatments against various diseases, such as diabetes, cancer, or heart diseases. However, the limited availability of polyphenols represents a major obstacle to clinical applications that must be overcome. In comparison to the quantities of these compounds obtained by isolation from natural sources or costly chemical synthesis, the microbial production of these compounds could provide sufficient quantities from inexpensive substrates. In this work, we describe the development of an *Escherichia coli* platform strain for the production of pinosylvin, a stilbene found in the heartwood of pine trees which could aid in the treatment of various cancers and cardiovascular diseases. Initially, several configurations of the three-step biosynthetic pathway to pinosylvin were constructed from a set of two different enzymes for each enzymatic step. After optimization of gene expression and evaluation of different construct environments, low pinosylvin concentrations up to 3 mg/liter could be detected. Analysis of the precursor supply and a comparative analysis of the intracellular pools of pathway intermediates and product identified the limited malonyl coenzyme A (malonyl-CoA) availability and low stilbene synthase activity in the heterologous host to be the main bottlenecks during pinosylvin production. Addition of cerulenin for increasing intracellular malonyl-CoA pools and the *in vivo* evolution of the stilbene synthase from *Pinus strobus* for improved activity in *E. coli* proved to be the keys to elevated product titers. These measures allowed product titers of 70 mg/liter pinosylvin from glucose, which could be further increased to 91 mg/liter by the addition of L-phenylalanine.

Plant polyphenols are plant secondary metabolites which have important functions in plant defense and signaling or serve as pigments. Furthermore, many polyphenols have antioxidant, anticancer, and anti-inflammatory properties, rendering these metabolites an invaluable source of bioactive compounds for drug discovery and drug development in the pharmaceutical industry (1).

The polyphenol pinosylvin (*trans*-3,5-dihydroxystilbene) is a stilbene which can be predominantly found in the heartwood of conifer trees of the genus *Pinus* (2). Pinosylvin protects the plants against microbial and fungal decay (3), but it has also attracted attention due to its health benefits for humans. Several recent studies indicate a positive effect of pinosylvin in the treatment of various cancers (4, 5), cardiovascular inflammatory diseases (6), and adjuvant arthritis (7). Pinosylvin is synthesized from the aromatic amino acid L-phenylalanine in three enzymatic steps (Fig. 1) (8). L-Phenylalanine is first deaminated to *trans*-cinnamic acid by a phenylalanine ammonia lyase (PAL; EC 4.3.1.24). The resulting acid is subsequently coenzyme A (CoA) activated by a 4-coumarate-CoA ligase (4CL; EC 6.2.1.12), yielding the CoA thioester *trans*-cinnamoyl-CoA. A stilbene synthase (STS; EC 2.3.1.146), which is a type III polyketide synthase (PKS), catalyzes the successive condensation of three malonyl-CoA molecules with *trans*-cinnamoyl-CoA, forming a linear tetraketide intermediate. Finally, the STS also cyclizes the tetraketide intermediate via an intramolecular C-2 → C-7 aldol condensation to form the stilbene pinosylvin (8).

The concentration of pinosylvin in pine heartwood ranges from 1 to 40 mg/g (dry weight) (including its monomethyl ether) (3), rendering access to pinosylvin through extraction difficult. Furthermore, purification of pinosylvin from these extracts would require separation from a multitude of often structurally very similar compounds, such as other stilbenes or flavonoids (9). Various catalytic and noncatalytic chemical synthetic routes for the synthesis of stilbenes have been devised. However, these strategies suffer from the demand for expensive substrates, catalyst instability, or degradation or the formation of by-products and various isomers (10). In contrast, microbial production of pinosylvin from glucose would have the advantage of being much more environmentally friendly than chemical synthesis, since it avoids the use of organic solvents, heavy metals, and strong acids or bases. To date, several microorganisms have been engineered for microbial stilbene production, especially for the synthesis of resveratrol (11–13). However, stilbene production with these strains relies on the supplementation of phenylpropanoids (e.g., coumaric acid or cinnamic acid) as stilbene precursors. This strategy has led to some considerable success with regard to production of the stilbene resveratrol, where feeding of 15 mM *p*-coumaric acid resulted in maximum product titers of 1.4 g/liter in *Escherichia coli* (11), which could be further improved to 1.6 g/liter by increasing the carbon flux into malonyl-CoA (14). More recently, *E. coli* has also been engineered to produce 35 mg/liter resveratrol from 3 mM its

Received 12 September 2014 **Accepted** 12 November 2014

Accepted manuscript posted online 14 November 2014

Citation van Summeren-Wesenhagen PV, Marienhagen J. 2015. Metabolic engineering of *Escherichia coli* for the synthesis of the plant polyphenol pinosylvin. Appl Environ Microbiol 81:840–849. doi:10.1128/AEM.02966-14.

Editor: M. J. Pettinari

Address correspondence to Jan Marienhagen, j.marienhagen@fz-juelich.de.

Supplemental material for this article may be found at http://dx.doi.org/10.1128/AEM.02966-14.

doi:10.1128/AEM.02966-14

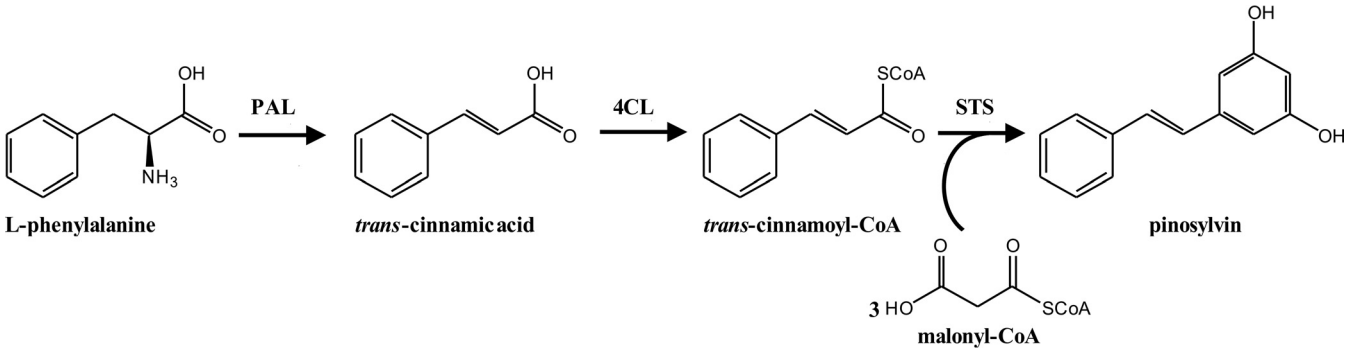

FIG 1 Biosynthetic pathway from L-phenylalanine to pinosylvin. Abbreviations: PAL, phenylalanine ammonia lyase; 4CL, 4-coumarate-CoA ligase; STS, stilbene synthase.

amino acid precursor L-tyrosine (15). This was achieved by following a modular metabolic engineering strategy for balancing the pathway with the *matB-matC* system from *Rhizobium trifolii*, which synthesizes the precursor malonyl-CoA from supplemented malonate. In comparison, product titers reported for pinosylvin are modest, with 0.6 mg/liter being achieved with *Streptomyces venezuelae* (when supplementing 1.2 mM *trans*-cinnamic acid) (16) and 155 mg/liter being achieved during biotransformation with *E. coli* (when providing 1 mM *trans*-cinnamic acid and augmenting intracellular malonyl-CoA levels) (17).

In this study, we examined multiple genes and pathway configurations for microbial pinosylvin production by *E. coli* from glucose. For this purpose, we optimized heterologous gene expression, examined precursor availability, and performed laboratory protein evolution to enhance the activity of a plant-derived STS in the microbial host.

MATERIALS AND METHODS

Bacterial strains, plasmids, and growth conditions. The bacterial strains and plasmids used or constructed in the course of this work are listed in Table 1. *E. coli* DH5α, solely used for cloning purposes, was routinely cultivated on a rotary shaker (170 rpm) at 37°C in LB medium or on LB plates (LB medium with 1.5% [wt/vol] agar) (18). If appropriate, carbenicillin (50 μg/ml), kanamycin (30 μg/ml), or spectinomycin (50 μg/ml) was added to the medium. Growth was determined by measuring the optical density at 600 nm (OD_{600}).

Recombinant DNA techniques. The enzymes for recombinant DNA work were obtained from Thermo Scientific (Waltham, MA, USA) and Merck Millipore (Billerica, MA, USA). Routine methods like PCR, restriction, or ligation were carried out according to standard protocols (18). Oligonucleotides used for cloning, error-prone PCR (epPCR), and site-directed mutagenesis (19) were obtained from Eurofins Genomics (Ebersberg, Germany) and are listed in Table 2. *E. coli* was transformed by the RbCl method (20). The PAL, 4CL, and STS genes were chemically synthesized by GeneArt Gene Synthesis Services from Life Technologies, a Thermo Fisher Scientific company (Waltham, MA, USA). Genes were codon optimized for expression in *E. coli* by employing the proprietary GeneOptimizer software. For subcloning purposes, all PAL and STS genes were synthesized with a 5′ NcoI restriction site and a 3′ BamHI restriction site, whereas the synthetic 4CL genes incorporate a 5′ NdeI site and a 3′ XhoI site. The 5′ NdeI and 5′ NcoI restriction sites already include the start codon ATG as part of the recognition sites. However, in the case of the *sts2* gene from *Pinus strobus*, subcloning using the NcoI site required the addition of the glycine codon GGA after the start codon since the NcoI recognition site (5′-CCATGG-3′) comprises a G following the start ATG codon.

Heterologous gene expression. Recombinant *E. coli* BL21(DE3) strains expressing genes for the pinosylvin synthetic pathway were cultivated in 25 ml LB medium in 100-ml baffled shake flasks at 37°C and 120 rpm until an OD_{600} of 0.6 was reached. After induction with 1 mM isopropyl-β-D-thiogalactopyranoside (IPTG), the cultivation continued at 30°C for 24 h. Cells were then harvested by centrifugation (3,900 × *g*, 15 min, 4°C) and washed with 5 ml 0.9% (wt/vol) NaCl solution. After centrifugation (3,900 × *g*, 15 min, 4°C), the cells were resuspended in 1 ml phosphate-buffered saline (1.9 mM NaH_2PO_4, 8.1 mM Na_2HPO_4, 154 mM NaCl, pH 7.4) and disrupted by sonication using a Branson sonifier 250 (intensity, 2; duty cycle, 20%; 4 min; Branson, Danbury, CT, USA). After removal of the cellular debris by centrifugation (16,000 × *g*, 30 min, 4°C), the cell extract (CE) was subjected to SDS-PAGE analysis using NuPAGE bis-Tris gels from Life Technologies (Waltham, MA, USA).

For purification of the His_6-tagged STS proteins, *E. coli* BL21(DE3) cultures were cultivated in 100 ml LB medium in 500-ml baffled shake flasks on a rotary shaker (120 rpm) at 37°C until an OD_{600} of 0.2 was reached. The cultures were shifted to 30°C, and gene expression was induced with 0.1 mM IPTG as soon as an OD_{600} of 0.6 was reached. After 4 h, the cells were harvested by centrifugation (6,200 × *g*, 10 min, 4°C) and washed with an ice-cold 0.9% (wt/vol) NaCl solution. After centrifugation (6,200 × *g*, 10 min, 4°C), the cells were resuspended in 1 ml NNI10 lysis buffer (50 mM NaH_2PO_4, 300 mM NaCl, 10 mM imidazole, pH 8) and subsequently disrupted by sonication (intensity, 2; duty cycle, 20%; 4 min). The resulting CE was clarified by centrifugation (16,000 × *g*, 30 min, 4°C). A column volume (CV) of 1 ml nickel-nitrilotriacetic acid resin (Qiagen, Hilden, Germany) was used for protein purification. After equilibration of the column by applying 5 CVs of NNI10 buffer, the CE was loaded on the column. Subsequently, the column was washed three times with 10 CVs of NNI70 wash buffer (50 mM NaH_2PO_4, 300 mM NaCl, 70 mM imidazole, pH 8). The elution of the STS proteins was achieved by applying 1 CV of NNI250 elution buffer (50 mM NaH_2PO_4, 300 mM NaCl, 250 mM imidazole, pH 8) six times. The eluted fractions were analyzed by SDS-PAGE.

Furthermore, the successful expression of all PAL, 4CL, and His-STS proteins was verified by matrix-assisted laser desorption ionization–time of flight (MALDI-TOF) mass spectrometry (MS) as previously described (21).

Pinosylvin production with *E. coli*. Recombinant *E. coli* BL21(DE3) strains were cultivated either in 50 ml LB broth or in 50 ml yeast nitrogen base (YNB) defined medium in 500-ml baffled shake flasks on a rotary shaker (120 rpm) at 26°C. For the preparation of 1 liter of YNB medium, 100 ml of 10-times-concentrated YNB was added to 900 ml base medium [6 g K_2HPO_4, 3 g KH_2PO_4, 10 g 3-(*N*-morpholino)propanesulfonic acid (MOPS), pH 7], and 5 g/liter glucose was added as a carbon source. Precultures were cultivated overnight at 37°C (170 rpm) in LB or YNB medium and then diluted to an OD_{600} of 0.1 in 50 ml fresh LB or YNB

TABLE 1 Strains and plasmids used in this study

Strain or plasmid	Relevant characteristics	Source
Strains		
E. coli DH5α	F^- ϕ80d*lacZ*ΔM15 Δ(*lacZYA-argF*)*U169 recA1 endA1 hsdR17*(r_K^- m_K^+) *phoA supE44 thi-1 gyrA96 relA1* λ^-	Invitrogen (Karlsruhe, Germany)
E. coli BL21(DE3)	F^- *ompT hsdSB*(r_B^- m_B^-) *gal dcm* (DE3)	Invitrogen (Karlsruhe, Germany)
Plasmids		
pCDFDuet1	Spt^r; 2× T7 *lac* promoters, CDF replicon, *lacI*, His_6 tag, S tag	Merck Millipore (Billerica, MA, USA)
pETDuet1	Amp^r; 2× T7 *lac* promoters, ColE1 replicon, *lacI*, His_6 tag, S tag	Merck Millipore (Billerica, MA, USA)
pRSFDuet1	Kan^r; 2× T7 *lac* promoters, RSF replicon, *lacI*, His_6 tag, S tag	Merck Millipore (Billerica, MA, USA)
pUC18	Amp^r; pMB1 replicon, P*lac lacI*, containing the 5′ terminal part of the *lacZ* gene encoding the N-terminal fragment of beta-galactosidase	Merck Millipore (Billerica, MA, USA)
pE-*Pcpal1*	pETDuet1 derivative containing *pal1* from *P. crispum*	This study
pE-*Atpal2*	pETDuet1 derivative containing *pal2* from *A. thaliana*	This study
pC-*Pdsts3-Sc4cl*	pCDFDuet1 derivative containing *sts3* from *P. densiflora* and *4cl A294G* from *S. coelicolor*	This study
pC-*Pdsts3-At4cl2*	pCDFDuet1 derivative containing *sts3* from *P. densiflora* and *4cl2 N256A/M293P/K320L* from *A. thaliana*	This study
pC-*Pstrsts2-Sc4cl*	pCDFDuet1 derivative containing *sts2* from *P. strobus* and *4cl A294G* from *S. coelicolor*	This study
pC-*Pstrsts2-At4cl2*	pCDFDuet1 derivative containing *sts2* from *P. strobus* and *4cl2 N256A/M293P/K320L* from *A. thaliana*	This study
pR-*Pstrsts2*	pRSFDuet1 derivative containing *sts2* from *P. strobus*	This study
pR-*HisPdsts3*	pRSFDuet1 derivative containing *sts3* from *P. densiflora* with an N-terminal His_6 tag	This study
pR-*HisPstrsts2*	pRSFDuet1 derivative containing *sts2* from *P. strobus* with an N-terminal His_6 tag	This study
pE-*Pcpal1-Sc4cl*	pETDuet1 derivative containing *pal1* from *P. crispum* and *4cl A294G* from *S. coelicolor*	This study
pE-*Pcpal1-At4cl2*	pETDuet1 derivative containing *pal1* from *P. crispum* and *4cl2 N256A/M293P/K320L* from *A. thaliana*	This study
pE-*Atpal2-Sc4cl*	pETDuet1 derivative containing *pal2* from *A. thaliana* and *4cl A294G* from *S. coelicolor*	This study
pE-*Atpal2-At4cl2*	pETDuet1 derivative containing *pal2* and *4cl2 N256A/M293P/K320L* from *A. thaliana*	This study
pUC18-P*gap-HisPstrsts2-Sc4cl-Pcpal1*	pUC18 derivative containing *sts2* from *P. strobus* with an N-terminal His_6 tag, *4cl A294G* from *S. coelicolor*, and *pal1* from *P. crispum* organized as an operon under the control of the promoter P*gap*	This study
pR-*HisPstrsts2-Sc4cl-Pcpal1*	pRSFDuet1 derivative containing *sts2* from *P. strobus* with an N-terminal His_6 tag, *4cl A294G* from *S. coelicolor*, and *pal1* from *P. crispum* organized as an operon	This study
pR-T7-*accBC*-T7-*dtsR1*	pRSFDuet1 derivative containing *accBC* and *dtsR1*, encoding the biotin-containing α subunit and core catalytic β subunit, respectively, from ACC of *C. glutamicum*	This study
pE-*fabF*	pETDuet1 derivative containing β-ketoacyl-ACP synthase II or FabF from *E. coli* BL21(DE3)	This study
pR-*HisPstrsts2T248A-Sc4cl-Pcpal1*	pRSFDuet1 derivative containing *sts2 T248A* from *P. strobus* with an N-terminal His_6 tag, *4cl A294G* from *S. coelicolor*, and *pal1* from *P. crispum* organized as an operon	This study
pR-*HisPstrsts2Q361R-Sc4cl-Pcpal1*	pRSFDuet1 derivative containing *sts2 Q361R* from *P. strobus* with an N-terminal His_6 tag, *4cl A294G* from *S. coelicolor*, and *pal1* from *P. crispum* organized as an operon	This study
pR-*HisPstrsts2T248A/Q361R -Sc4cl-Pcpal1*	pRSFDuet1 derivative containing *sts2 T248A/Q361R* from *P. strobus* with an N-terminal His_6 tag, *4cl A294G* from *S. coelicolor*, and *pal1* from *P. crispum* organized as an operon	This study

TABLE 2 Oligonucleotides used in this study

Purpose and oligonucleotide	Sequence (5′ → 3′) and properties[a]
Cloning of His_6-tagged stilbene synthases	
F_BamHI_PdSTS3	GGATCCAATGGGTGGTGTTGATTTTGAAGGTTTTCG (BamHI)
R_NotI_PdSTS3	GCGGCCGCTTATTACGGATGACAGGTAC (NotI)
F_BamHI_PstrSTS2	GGATCCAATGGGAAGCGTTGGTATGGGTG (BamHI)
R_NotI_PstrSTS2	GCGGCCGCTTATTACGGAAACGGAATGC (NotI)
Construction of pinosylvin operon under control of T7 promoter	
F_Sc4CL_NotI	CGCAGTGCGGCCGCGAAAGGAGGTCTATATGTTTCGTAGCGAATATGC (NotI)
R_Sc4CL	CGCAGTGGTACCCGCATAGTACTTTATTAACGCGGTTCACGCAG (KpnI/ScaI)
F_PcPAL1	CGCAGTGGTACCGAAAGGAGGTCTATATGGAAAATGGTAATGGTGCAAC (KpnI)
R_PcPAL1_XhoI	CGCAGTCTCGAGTTATTAACAAATCGGCAGCGGTGCACCATTCCAG (XhoI)
Construction of pinosylvin operon under control of P_{GAPDH} promoter	
F_P_{GAPDH}_NdeI	CGCCATATGGATCAAACAGTGATATACGCCGTCAC (NdeI)
R_P_{GAPDH}_HindIII	CGCAAGCTTATATTCCACCAGCTATTTGTTAGTGAATAAAAGG (HindIII)
F_HisPstrSTS2_SalI	CGCAGTGTCGACAAGGAGATATACCATGGGCAGCAGCCATCACCATC (SalI)
R_HisPstrSTS2_NheI	CGCATGCTAGCTTATTACGGAAACGGAATGCTTTTCAGCACAAC (NheI)
F_Sc4CL	CGCAGTGGATCCGAAAGGAGGTCTATATGTTTCGTAGCGAATATGCAG (BamHI)
R_Sc4CL	CGCAGTGGTACCCGCATAGTACTTTATTAACGCGGTTCACGCAG (KpnI/ScaI)
F_PcPAL1	CGCAGTGGTACCGAAAGGAGGTCTATATGGAAAATGGTAATGGTGCAAC (KpnI)
R_PcPAL1	CGCAGTGAATTCTTATTAACAAATCGGCAGCGGTG (EcoRI)
Construction of pR-T7-*accBC*-T7-*dtsR1*	
F_accBC_BamHI	CGCAGTGGATCCTGTCAGTCGAGACTAGGAAGATCACCAAG (BamHI)
R_accBC_HindIII	CGCAGTAAGCTTTTATTACTTGATCTCGAGGAGAACAACGC (HindIII)
F_dtsR1_NdeI	CGCAGTCATATGATGACCATTTCCTCACCTTTGATTGACGTCGCCAACC (NdeI)
R_dtsR1_XhoI	CGCAGTCTCGAGTTATTACAGTGGCATGTTGCCGTGCTTG (XhoI)
Construction of pE-*fabF*	
F_fabF_NcoI	CGCAGTCCATGGGTGTCTAAGCGTCGTGTAGTTGTG (NcoI)
R_fabF_EcoRI	CGCAGTGAATTCGCAGCATGTTCACTACGGAACAAGTC (EcoRI)
PstrSTS3 epPCR	
F_PstrSTS2_Ep	CGCAGTGGATCCAATGGGAAGCGTTGGTATGGGTG (BamHI)
R_PstrSTS2_Ep	CGCAGTGCGGCCGCTTATTACGGAAACGGAATGC (NotI)
Site-directed mutagenesis at Q361 of PstrSTS3	
F_Q361R	CGTAAAGCAAGCCGTCGGAATGGTTGTAGCACC
R_Q361R	GGTGCTACAACCATTCCGACGGCTTGCTTTACG

[a] Recognition sites for the indicated restriction enzymes are underlined.

medium, respectively. When the OD_{600} of these main cultures reached 0.6, gene expression was induced with 1 mM IPTG (when necessary), and the cultivation was continued for 36 h at 26°C. Samples were taken at regular time intervals for liquid chromatography (LC)-MS analysis to follow the formation of pinosylvin.

A two-stage cultivation procedure was also employed for pinosylvin production. In the first stage, cultivation and gene expression were performed in LB as described above. After 5 h of heterologous gene expression, cells were collected by centrifugation (4,300 × *g*, 15 min, 4°C) and subsequently resuspended in 10 ml YNB medium–5 g/liter glucose, which was supplemented with 1 mM IPTG. The cultivation of this second phase was continued for 36 h at 26°C. Again, samples were taken at regular time intervals for LC-MS analysis.

Metabolite extraction. Metabolite extracts from supernatants and cells were prepared for LC-MS analysis by mixing 1 ml culture with 1 ml ethyl acetate and vigorous shaking (1,400 rpm, 10 min, 20°C) in an Eppendorf thermomixer (Hamburg, Germany). This suspension (800 μl) was centrifuged for 5 min at 16,000 × *g*, and the ethyl acetate layer was transferred to an organic solvent-resistant deep-well plate (Eppendorf, Hamburg, Germany). After evaporation of the ethyl acetate, 100 μl acetonitrile was added prior to LC-MS analysis, and this concentrated the extract 8-fold.

Determination of cytoplasmic metabolite concentrations. *E. coli* cells were separated from the medium and inactivated by silicone oil centrifugation for the determination of cytoplasmic concentrations of *trans*-cinnamic acid, *trans*-cinnamoyl CoA, malonyl-CoA, and pinosylvin as described previously (22). The resulting upper phase was used for further analysis by LC-MS/MS.

Chemical synthesis of *trans*-cinnamoyl-CoA. *trans*-Cinnamic acid was esterified in the presence of CoA and dicyclohexyl carbodiimide as previously described to prepare a standard for the LC-MS/MS analysis of *trans*-cinnamoyl-CoA (23). All required chemicals were purchased from Sigma-Aldrich (St. Louis, MO, USA).

Determination of intermediates and pinosylvin by LC-MS and LC-MS/MS. The *trans*-cinnamic acid and pinosylvin in the cell-free culture medium as well as in the ethyl acetate-extracted samples were quantified by LC-MS using an ultra-high-performance LC (uHPLC) 1290 Infinity system coupled to a 6130 quadrupole LC-MS system (Agilent, Santa

Clara, CA, USA). LC separation was carried out with a Kinetex 1.7u C_{18} 100-Å-pore-size column (50 mm by 2.1 mm [internal diameter]; Phenomenex, Torrance, CA, USA) at 50°C. For elution, 0.1% acetic acid (solvent A) and acetonitrile supplemented with 0.1% acetic acid (solvent B) were applied as the mobile phases at a flow rate of 0.5 ml/min. A gradient was used, where solvent B was increased stepwise (minute 0 to 1, 15% to 22%; minute 1 to 2, 22% to 40%; minute 2 to 2.5, 40% to 50%; minute 2.5 to 3, 50% to 100%). The mass spectrometer was operated in the negative electrospray ionization (ESI) mode, and data acquisition was performed in selected-ion-monitoring mode. LC-MS/MS was used for the quantification of *trans*-cinnamic acid, *trans*-cinnamoyl-CoA, malonyl-CoA, and pinosylvin in the cytoplasmic extracts following a previously described method (24). *trans*-Cinnamic acid, malonyl-CoA, and pinosylvin standards were purchased from Sigma-Aldrich (St. Louis, MO, USA).

Construction of *Pstrsts2* epPCR libraries and microtiter plate screening for increased pinosylvin production. All epPCRs of the *sts2* gene from *P. strobes* (*Pstrsts2*), with mutation rates varying from 2 to 4.6 mutations/kb, were performed using a Diversify PCR random mutagenesis kit from Clontech (Mountain View, CA, USA). The mutated *Pstrsts2* genes were subcloned into the pRSFDuet1 backbone carrying the genes for PAL isozyme 1 from *Petroselinum crispum* PAL1 (PcPAL1) and 4CL from *Streptomyces coelicolor* (Sc4CL), resulting in the vector pR-*His Pstrsts2*-Sc4cl-Pcpal1*, and this vector was transformed into *E. coli* BL21(DE3). At least 90 clones for each mutation rate, always accompanied by a negative control [*E. coli* BL21(DE3)/pRSFDuet1] and a strain expressing the wild-type *sts2* gene [*E. coli* BL21(DE3)/pR-*HisPstrsts2-Sc4cl-Pcpal1*], were screened for improved pinosylvin titers. For this purpose, cultivation and screening were performed in the 96-well microtiter plate format. The libraries were cultivated in 600 μl YNB medium supplemented with 5 g/liter glucose, 3 mM L-phenylalanine, 0.5 mM IPTG, and 30 μg/ml kanamycin in deep-well plates from Eppendorf (Hamburg, Germany) and a Microtron shaker from Infors (Bottmingen, Switzerland) at 30°C, 900 rpm, and 75% humidity for 24 h. Subsequently, 100 μl culture from each well was transferred to a UV-transparent 96-well flat-bottom plate from Corning (Corning, NY, USA). An Infinite M200 Pro microplate reader (Tecan, Männedorf, Switzerland) was used to compare relative pinosylvin titers on the basis of the fluorescent properties of pinosylvin (excitation $\lambda = 316$ nm, emission $\lambda = 388$ nm).

RESULTS

Design of a synthetic pathway for pinosylvin. For the construction of a synthetic pinosylvin pathway, we first consulted the recent literature and the BRaunschweig ENzyme DAtabase (BRENDA) to identify suitable phenylalanine ammonia lyases (PALs), 4-coumarate-CoA ligases (4CLs), and stilbene synthases (STSs) originating from either plants or microorganisms (25). Enzymes were considered suitable if they had already been functionally expressed in *E. coli* and if the determined basic catalytic parameters (e.g., k_{cat}, K_m) appeared to be promising for the construction of an efficient route toward the biosynthesis of pinosylvin. In the course of that survey, we selected PAL isozyme 1 from *Petroselinum crispum* (PcPAL1) and PAL isozyme 2 from *Arabidopsis thaliana* (AtPAL2), since both enzymes are characterized by high levels of activity when expressed in *E. coli*. Furthermore, we decided to express a variant of a 4CL-like enzyme from the Gram-positive bacterium *Streptomyces coelicolor* (Sc4CL), which favors *trans*-cinnamic acid over *p*-coumaric acid as the substrate, and a variant of 4CL isozyme 2 of *Arabidopsis thaliana* (At4CL2). As candidates for stilbene synthases, we selected STS isozyme 3 of *Pinus densiflora* (PdSTS3) and STS isozyme 2 of *Pinus strobus* (PstrSTS2), as these isozymes were reported to have high specificity and activity toward cinnamoyl-CoA.

Optimization of heterologous gene expression. For initial gene expression experiments, all PAL genes were cloned into the pETDuet1 vector, whereas the STS and 4CL genes were cloned into pCDFDuet1 vector under the individual control of a T7 promoter. The successful expression of soluble protein could be verified for all PALs and 4CLs by SDS-PAGE analysis. However, no visible bands indicating successful expression of PdSTS3 or PstrSTS2 could be observed in the soluble or the insoluble protein fractions (data not shown). Neither an incremental reduction of the expression temperature from 30°C to 15°C nor variation of the IPTG concentration (0.4 mM to 1 mM) improved STS expression. Furthermore, a first analysis of the supernatant of the expression cultures showed that up to 1.7 mM *trans*-cinnamic acid but no pinosylvin was produced by the recombinant *E. coli* strains. In order to improve the expression of PdSTS3 and PstrSTS2, the genes for both were individually cloned into the pRSFDuet1 vector, another member of the pDuet vector family bearing the origin of replication from the plasmid RSF1030, which allows for a higher number of plasmid copies per cell (>100 copies per cell). In addition, both genes were cloned with an N-terminal His_6 tag, since such a tag improved the soluble expression of PdSTS3 without affecting the activity of STS in *in vitro* enzyme assays (26). Despite these alterations, no soluble STS expression was observable in CEs, but both His_6-tagged enzymes (HisPstrSTS2 and HisPdSTS3) could be identified in the whole-cell fraction. Purification of the enzymes from the CE by affinity chromatography finally revealed a low level of expression of soluble HisPstrSTS2 protein but not HisPdSTS3 in the CE (see Fig. S1 in the supplemental material). Possibly, native *E. coli* proteins concealed the band corresponding to HisPstrSTS2 on SDS-PAGE analysis of the CE. Finally, the identity of all PALs, 4CLs, and HisSTS proteins was confirmed by MALDI-TOF MS (data not shown). The accompanying chemical analysis of the cultures during the optimization of heterologous gene expression revealed that the modification of STS expression already resulted in the accumulation of low concentrations of pinosylvin (0.068 ± 0.004 mg/liter), but only in extracts of strains expressing HisSTS of *P. strobus*.

Identification of the most suitable pathway configuration. After the identification of His_6-tagged PstrSTS2 as the only functional STS in *E. coli*, four different synthetic pathways with all combinations of the available PALs and 4CLs were constructed. Subsequently, the pinosylvin production of all four strains was compared using the two-phase cultivation conditions described in Materials and Methods. As it turned out, the combination of the PAL from *P. crispum*, the 4CL from *S. coelicolor*, and the STS from *P. strobus* proved to be the most productive pathway variant, but only a low product concentration of up to 0.64 mg/liter pinosylvin could be detected (Table 3). Interestingly, the combination of PcPAL1 and At4CL2 did not lead to any detectable product formation, even though both enzymes functioned in other pathway configurations. The positive effect of the His_6 tag on PstrSTS2 expression was also reflected by increased pinosylvin titers, as the same strain expressing PstrSTS2 without the His_6 tag accumulated only up to 0.22 mg/liter pinosylvin (Table 3).

At this point, all genes of the pinosylvin pathway were expressed under the control of their own T7 promoter to rule out any polar expression effects. With the aim of evaluating the expression of the pathway from a single three-gene operon, two additional plasmids were constructed in which the operon was expressed under the control of either the IPTG-inducible T7 pro-

TABLE 3 Pinosylvin production with *E. coli* strains harboring different variants of the pinosylvin pathway in mono- or tricistronic transcriptional units

Strain	Pinosylvin titer (mg/liter)	
	Expt no. 1	Expt no. 2
E. coli BL21(DE3)/pE-*Pcpal1-Sc4cl*/pR-*HisPstrsts2*	0.49	0.64
E. coli BL21(DE3)/pE-*Pcpal1-At4cl2*/pR-*HisPstrsts2*	—[a]	—
E. coli BL21(DE3)/pE-*Pcpal1-Sc4cl*/pR-*Pstrsts2*	0.21	0.22
E. coli BL21(DE3)/pE-*Atpal2-Sc4cl*/pR-*HisPstrsts2*	0.27	0.36
E. coli BL21(DE3)/pE-*Atpal2-At4cl2*/pR-*HisPstrsts2*	0.24	0.31
E. coli BL21(DE3)/pUC18-P*gap-HisPstrsts2-Sc4cl-Pcpal1*	—	—
E. coli BL21(DE3)/pR-*HisPstrsts2-Sc4cl-Pcpal1*	3.21	3.37

[a] —, the titer was below the limit of detection.

moter (using the pRSFDuet1 vector backbone) or the constitutive *gap* promoter (P*gap*) of the glyceraldehyde-3-phosphate dehydrogenase (GAPDH) from *E. coli* (using the pUC18 vector backbone) (27). The *gap* promoter was selected, as it induces gene expression during cultivation on glucose as the carbon source, thus allowing the continuous transcription of the three heterologous genes. Surprisingly, no pinosylvin formation could be detected when the synthetic operon was constitutively expressed during single-phase cultivation in YNB supplemented with 5 g/liter glucose. Only the accumulation of up to 10 mg/liter *trans*-cinnamic acid during the cultivation could be measured. In contrast, IPTG-induced expression from the T7 promoter of the tricistronic pRSFDuet1 construct led to a 6-fold increased pinosylvin titer with *E. coli* BL21(DE3)/pR-*HisPstrsts2-Sc4cl-Pcpal1* (up to 3.37 mg/liter) compared to that achieved with the monocistronic organization of the same genes in *E. coli* BL21(DE3)/pE-*Pcpal1-Sc4cl* pR-*His Pstrsts2* (Table 3).

Availability of precursors and intermediates during pinosylvin synthesis. At this stage, insufficient levels of the precursors L-phenylalanine and malonyl-CoA could be limiting for the overall product titers. In order to find out whether the availability of L-phenylalanine or malonyl-CoA was limiting, cultivations were performed in which 3 mM L-phenylalanine and/or cerulenin (up to 200 μM) was supplemented during the production phase (Fig. 2). Cerulenin is an antifungal antibiotic produced by *Cephalosporium caerulens*, which blocks fatty acid biosynthesis by inhibiting the β-ketoacyl-acyl carrier protein (ACP) synthases FabB and FabF, thereby preventing channeling of malonyl-CoA into the pathway for fatty acid synthesis (28). The exclusive supplementation of L-phenylalanine had no positive effect on pinosylvin production (3.29 ± 0.11 mg/liter without supplementation versus 3.49 ± 0.42 mg/liter with supplementation) but resulted in the accumulation of the intermediate *trans*-cinnamic acid in the supernatant (data not shown). In contrast, addition of cerulenin drastically increased product titers up to 18-fold, reaching 59 mg/liter pinosylvin at a concentration of 200 μM cerulenin (and no addition of L-phenylalanine).

Subsequently, the cytoplasmic levels of malonyl-CoA in *E. coli* BL21(DE3) were determined to verify that the addition of cerulenin had an effect on the intracellular malonyl-CoA pool. These experiments revealed that the intracellular malonyl-CoA level increased from 2 pmol/mg cell dry weight (CDW) (no cerulenin) to 105 pmol/mg CDW at 1.5 h after the addition of 200 μM cerulenin. In contrast, *E. coli* BL21(DE3)/pR-*HisPstrsts2-Sc4cl-Pcpal1* accumulated malonyl-CoA only up to 59 pmol/mg CDW in the presence of 200 μM cerulenin and during pinosylvin synthesis (see Fig. S2 in the supplemental material), indicating malonyl-CoA consumption during pinosylvin formation. L-Phenylalanine supplementation had a positive impact on product formation during cerulenin-mediated inhibition of fatty acid synthesis, indicating that the availability of this precursor becomes limiting when more malonyl-CoA is available (Fig. 2). At this stage, supplementation of 3 mM L-phenylalanine and addition of 200 μM cerulenin led to the highest pinosylvin titer of 70 mg/liter after 36 h of cultivation.

Two additional strategies for improving the intracellular malonyl-CoA availability in *E. coli* to circumvent cerulenin addition were pursued: overexpression of the intrinsic β-ketoacyl-ACP synthase II (FabF) for reducing the drain of malonyl-CoA into fatty acid synthesis, as well as heterologous expression of the acetyl-CoA carboxylase (ACC) from *Corynebacterium glutamicum* for increasing the intracellular generation of malonyl-CoA from acetyl-CoA. Unfortunately, heterologous expression of either enzyme led only to reduced pinosylvin titers (data not shown).

The availability of the intermediate *trans*-cinnamoyl-CoA during pinosylvin synthesis could also be limiting due to low 4CL activity. Therefore, the relative intracellular levels of *trans*-cinnamic acid, *trans*-cinnamoyl-CoA, and pinosylvin were determined during cultivation with 3 mM L-phenylalanine and with and without addition of cerulenin in the production phase (Fig. 3). During these experiments, L-phenylalanine was always supplemented to ensure that *trans*-cinnamic acid, as the direct precursor of *trans*-cinnamoyl-CoA, was not limiting in the presence of cerulenin. All measurements were conducted 2 h after addition of cerulenin, but only the relative levels of intermediates and product could be determined, since no *trans*-cinnamoyl-CoA standard of sufficient purity could be chemically synthesized. As a result, addition of 200 μM cerulenin led to an 18-fold increase of pinosylvin, accompanied by a drop of the *trans*-cinnamoyl-CoA level of only 30%. This observation hints that the levels of *trans*-cinnamoyl-CoA are sufficient to achieve higher product titers, as the pool of this intermediate is not depleted or even significantly reduced.

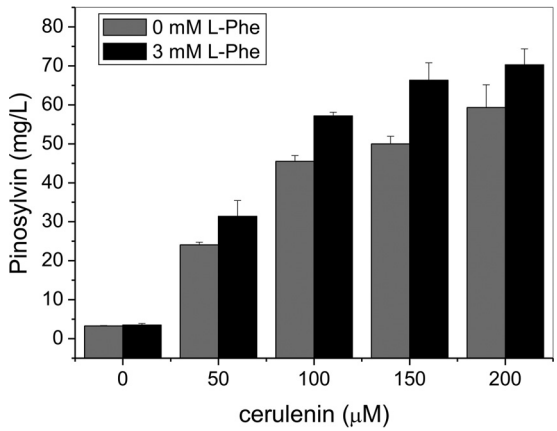

FIG 2 Pinosylvin production of *E. coli* BL21(DE3)/pR-*HisPstrsts2-Sc4cl-Pcpal1* with and without supplementation of L-phenylalanine and/or addition of cerulenin. The experiments were performed in triplicate.

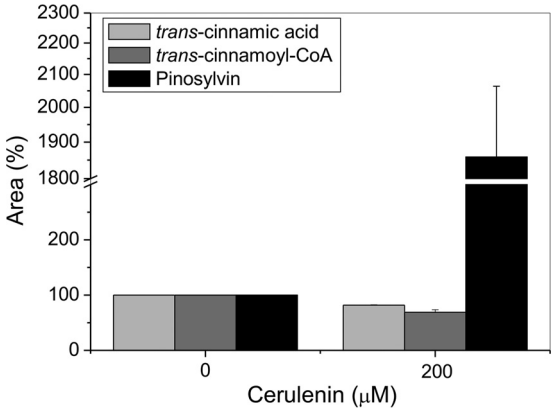

FIG 3 Relative intracellular levels of *trans*-cinnamic acid, *trans*-cinnamoyl-CoA, and pinosylvin determined by LC-MS/MS. The experiments with *E. coli* BL21(DE3)/pR-*HisPstrsts2-Sc4cl-Pcpal1* were performed in duplicate with supplementation of 3 mM L-phenylalanine and 0 μM or 200 μM cerulenin. The relative levels are given as the area (percent), with the areas for the intermediates determined with 0 μM cerulenin being set equal to 100%.

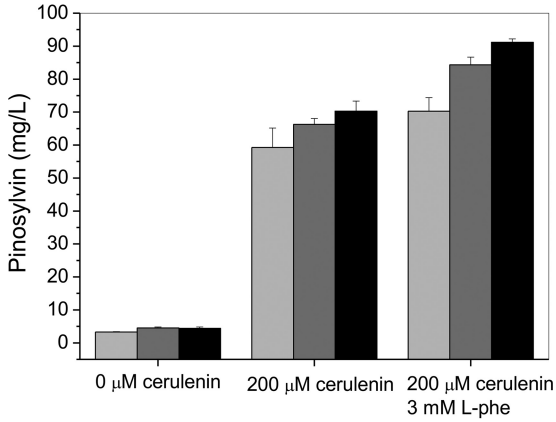

FIG 4 Comparison of the pinosylvin titers of *E. coli* BL21(DE3)/pR-*His Pstrsts2-Sc4cl-Pcpal1* expressing either wild-type *HisPstrsts2* (light gray bars), *HisPstrsts2* with the Q361R substitution (dark gray bars), or *HisPstrsts2* with the T248A substitution (black bars) without any supplementation, with addition of 200 μM cerulenin, or with addition of 200 μM cerulenin and supplementation of 3 mM L-phenylalanine. The experiments were performed in duplicate.

Directed protein evolution of HisPstrSTS2. The PAL and 4CL activity in *E. coli* appeared to be sufficient to support higher product titers, as the intracellular pools of *trans*-cinnamic acid and *trans*-cinnamoyl-CoA were not depleted during pinosylvin production. In contrast, expression of the STS was still low, even though the sequences of all STS genes were optimized for expression in *E. coli* prior to gene synthesis. Hence, the poor soluble expression of HisPstrSTS2 in the microbial host might be limiting the performance of the pinosylvin pathway. With the aim to adapt the STS2 of *P. strobus* for optimal expression in *E. coli*, we performed directed evolution of the HisPstrSTS2 *in vivo*. For this purpose, we randomly mutated the codon-optimized open reading frame of *HisPstrsts2* by epPCR and subcloned the resulting STS library into pR-*Sc4cl-Pcpal* to complete the pinosylvin pathway. Cultivation and screening of the library were performed in the microtiter plate (MTP) format, taking advantage of the fluorescence of pinosylvin for identifying clones with increased product titers in comparison to the titer of the starting strain, *E. coli* BL21(DE3)/pR-*His Pstrsts2-Sc4cl-Pcpal1*. Screening of 450 clones yielded 2 clones exhibiting a higher fluorescence under screening conditions. DNA sequencing revealed that each STS gene carries a single point mutation (A742G and A1082G), both of which lead to amino acid substitutions (T248A and Q361R, respectively). After recloning of the STS variants and retransformation to exclude any effect of the plasmid or strain background, the product titers of both variants were compared to the titer of the starting strain using the optimized cultivation conditions with and without the addition of cerulenin or the supplementation of L-phenylalanine.

Under all cultivation conditions tested, both amino substitutions in HisPstrSTS2 individually improved the overall product titers (Fig. 4). In a direct comparison, the positive effect of T248A for pinosylvin formation was more pronounced, as more pinosylvin could be detected in the extracts. In the presence of cerulenin, but without supplementation of L-phenylalanine, 70 mg/liter pinosylvin accumulated in the *E. coli* BL21(DE3)/pR-*HisPstrsts2T248A-Sc4cl-Pcpal1* cultures, whereas an additional supplementation of 3 mM L-phenylalanine increased the pinosylvin titer to 91 mg/liter. However, use of the combination of both amino acid substitutions in an attempt to further boost product formation failed and most likely resulted in an inactive STS variant, as no pinosylvin synthesis of *E. coli* BL21(DE3)/pR-*HisPstrsts2T248A/Q361R-Sc4cl-Pcpal1* was detected.

DISCUSSION

The development of efficient microbial platform organisms for the production of (plant) natural products requires the identification of suitable enzymes, the design of stable genetic constructs for gene expression, and the optimal adaptation of the synthetic pathway to the host cell metabolism (or vice versa). In this work, we systematically explored several strategies to engineer *E. coli* for the microbial production of the stilbene pinosylvin. The efforts included the optimization of gene expression conditions, the comparison of different expression constructs, and protein engineering to adapt the expression of the plant-derived STS2 from *P. strobus* to the microbial host system.

Since construction of stilbene-producing microorganisms has mostly been limited to strains requiring the supplementation of phenylpropanoid intermediates, we decided to design and implement the complete three-step pathway to pinosylvin starting from the amino acid L-phenylalanine. We set off with the identification of the most suitable enzymes from various microbial or plant sources in the literature and databases and selected two enzymes for each of the three required enzymatic steps based on their kinetic properties. PALs, catalyzing the first committed step toward phenylpropanoid synthesis, can be found in all higher plants but are also present in yeasts, fungi, and some prokaryotic species (29). PAL isozyme 1 from *Petroselinum crispum* (PcPAL1) and PAL isozyme 2 from *Arabidopsis thaliana* (AtPAL2) were selected for the construction of the pinosylvin pathway since both enzymes are characterized by high levels of activity when expressed in *E. coli* (30, 31). In comparison to PALs, 4CLs are specific to the secondary metabolism of plants. Most 4CLs described are substrate specific, since all described natural substrates are characterized by a 4′-hydroxyl group on the phenyl ring (32). However, a synthetic

pathway leading to pinosylvin requires a CoA-ligase that accepts *trans*-cinnamic acid lacking this *para*-hydroxy moiety. Interestingly, Kaneko and coworkers discovered a bacterial 4CL-like enzyme from the filamentous, soil-dwelling, Gram-positive bacterium *Streptomyces coelicolor* (33). The enzyme showed a distinct 4CL activity, favoring *trans*-cinnamic acid over *p*-coumaric acid as the substrate. Mutational analysis of the substrate binding pocket indicated that the amino acid substitution A294G conferred even higher catalytic activity toward *trans*-cinnamic acid than the native enzyme. This particular enzyme variant (Sc4CL) was selected for evaluation in the synthetic pinosylvin pathway. The second 4CL candidate was a variant of 4CL isozyme 2 of *Arabidopsis thaliana* (At4CL2) bearing three amino acid substitutions (N256A, M293P, K320L). In *in vitro* enzyme assays, this mutein demonstrated a 30-fold higher level of conversion of *trans*-cinnamic acid than the native enzyme (34). Pinosylvin-forming stilbene synthases (EC 2.3.1.146) are typical for gymnosperms, and to date several such enzymes have been identified in three pine species, *Pinus sylvestris* (35), *Pinus densiflora* (26), and *Pinus strobus* (36). STS isozyme 3 of *P. densiflora* (PdSTS3) and STS isozyme 2 of *P. strobus* (PstrSTS2) were selected as STS candidates, as these isozymes were reported to have higher specificity and activity toward cinnamoyl-CoA than the other isozymes in *in vitro* enzyme assays (26, 36). Interestingly, compared to the other characterized STSs, PdSTS3 has a truncated C terminus, which is believed to be responsible for the observed release from feedback inhibition by pinosylvin (26).

The combination of PcPAL1 and Sc4CL in the synthetic pinosylvin pathway turned out to be more beneficial than the combination of AtPAL2 and Sc4CL to achieve high product titers. This is interesting, because At4CL2 performed better with AtPAL2 than with the PAL from *P. crispum*. This could simply be due to the common origin of both enzymes from *A. thaliana* but also supports the notion that the performance of an entire synthetic pathway instead of the performance of a pathway just assembled from individually characterized best parts should be evaluated. Pinosylvin production could be improved by organizing the three genes of the final pinosylvin pathway configuration in an operon under the control of a single promoter. The same effect was also observed during the development of a microbial production strain for resveratrol, where cotranscription of the genes for 4CLs and STSs was believed to lead to more balanced gene expression (11).

The availability of malonyl-CoA turned out to be crucial for the overall product titers, as the addition of the fatty acid production inhibitor cerulenin boosted the pinosylvin titers 18- to 20-fold, whereas the supplementation of L-phenylalanine alone had no effect. In order to avoid the addition of cerulenin, two strategies for increasing the availability of intracellular malonyl-CoA were followed: overexpression of the *E. coli* FabF (37) as well as heterologous expression of the ACC from *C. glutamicum*, as was successfully demonstrated during microbial polyketide synthesis and flavanone synthesis, respectively (17, 38, 39). However, none of these approaches had the desired effect, as pinosylvin production significantly decreased or ceased entirely. No improvement of microbial flavonoid production was also observed during microbial flavonoid production with *E. coli* upon expression of the ACC from *C. glutamicum*, suggesting that this strategy is not generally applicable (40). A comparative analysis of intracellular intermediate availability and product concentration in the presence or absence of 200 μM cerulenin was conducted, but the results obtained did not reveal a limiting enzymatic step when more malonyl-CoA was available. Additional experiments will be necessary to shed more light on this subject.

Finally, we performed directed protein evolution to adapt the expression of the pine-derived HisPstrSTS2 to the microbial host system. This was directly done in the genetic context of the pinosylvin pathway. Only one round of diversity generation by epPCR and MTP-based screening of 450 clones for increased pinosylvin-related fluorescence identified two clones, each bearing a single amino acid substitution, with improved product formation. The combination of both mutations had a detrimental effect on product formation, but the T248A substitution alone increased the final pinosylvin titer of the best strain, *E. coli* BL21(DE3)/pR-*His-Pstrsts2-Sc4cl-Pcpal1*, from 59 mg/liter to 70 mg/liter in the presence of 200 μM cerulenin and by an additional 30% to 91 mg/liter when L-phenylalanine was also supplemented. With the aim to understand the structural consequences of both amino acid substitutions, we generated a structure model for a PstrSTS2 dimer using the SWISS-MODEL server (41). A structure model for the pinosylvin synthase of *P. sylvestris* (PDB accession number 1U0U) (42), which was not among the pinosylvin synthases tested by us, served as the template for the calculated model since this enzyme shares 87% sequence identity to PstrSTS2 on the protein level. A structural alignment with structure models for the closely related chalcone synthase from *Medicago sativa* with coenzyme A bound (PDB accession number 1BQ6) (43) and the stilbene synthase from *Arachis hypogaea* with resveratrol bound (PDB accession number 1Z1F) (44) helped us to pinpoint the active site in the calculated PstrSTS2 model. Neither substitution is in close proximity to the assumed active sites of the PstrSTS2 dimer (Fig. 5A). T248 is located in the middle of a long β strand, and its side chain faces the interior of the protein at the dimer interface. The replacement by an L-alanine at this position could simply improve the flexibility of the protein and might ultimately lead to the observed improvement of STS activity in *E. coli*. In contrast, Q361 is positioned at the end of an α helix on the protein surface and located next to the amino acid sequence N362-G363-C364. This pattern follows the typical *N*-glycosylation sequence N-X-S/T/C of L-asparagine (*N*)-linked protein glycosylation, where X can be any amino acid except L-proline (45, 46). Analysis of the PstrSTS2 amino acid sequence with the web server GlycoEP also identified N362 to be a potential site for *N*-glycosylation in this particular STS (47). *E. coli* cannot perform L-asparagine *N*-linked protein glycosylation. Hence, replacement of L-glutamine with the more hydrophilic L-arginine at position 361 might simply lead to an improved stability or solubility of PstrSTS2 in the absence of any glycosylation in the heterologous host. When both amino acid substitutions were combined, no pinosylvin synthesis could be observed, suggesting that this enzyme variant is inactive. The β strand, in which T248 is located, is adjacent to the C-terminal β strand of PstrSTS2, and the α helix of Q361 interacts indirectly with the same C-terminal β strand via a loop (Fig. 5B). Possibly, the combination of both mutations simply destabilizes the architecture of PstrSTS2, rendering this enzyme variant inactive.

The key to success for the microbial production of pinosylvin from glucose without supplementation of any phenylpropanoid intermediate was the use of a combination of various metabolic engineering approaches and protein engineering of a heterologously expressed key enzyme. However, at this point the addition of cerulenin is still required for achieving significant product ti-

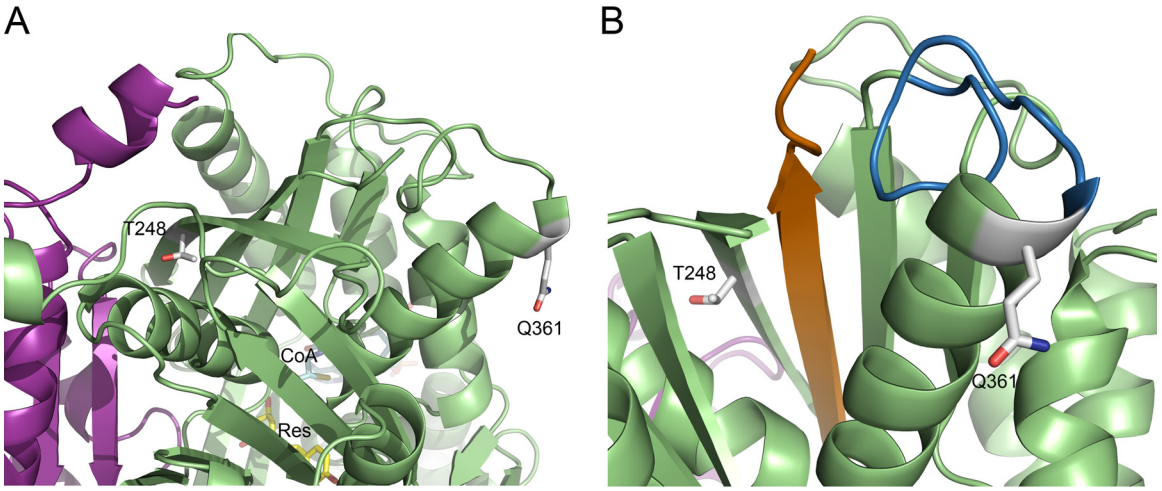

FIG 5 (A) Cartoon representation of a close-up of the pinosylvin synthase STS2 from *P. strobus*. The structure model was calculated using the model of the pinosylvin synthase of *P. sylvestris* as the template. The monomers are shown in green and purple, and the resveratrol (Res) and coenzyme A (CoA) highlighted in one monomer are shown in the stick mode in yellow and cyan/orange, respectively. T248 is located at the dimer interface, whereas Q361 is located on the protein surface. Both amino acids are shown in the stick mode. (B) Both T248 and Q361, shown in orange, interact with the C-terminal β strand. The β strand in which T248 is located is adjacent to this C-terminal β strand, and the α helix of Q361 interacts indirectly with the same C-terminal β strand via a loop.

ters. This could be circumvented by carrying out multiple genetic alterations of the central carbon metabolism to redirect the carbon flux to malonyl-CoA, as has been done for the microbial synthesis of the flavanone naringenin with *E. coli* (48). Here, the successful modifications suggested by the Optforce model included the overexpression of the genes for the pyruvate dehydrogenase multienzyme complex, phosphoglycerate kinase and acetyl-CoA carboxylase, and deletion of the genes encoding the fumarase and succinyl-CoA synthetase. Following this strategy, 5.6 times higher naringenin titers could be attained.

Nonetheless, protein engineering by directed evolution in the genetic context of the synthetic pathway, as presented here, could also be used to harmonize the entire pinosylvin pathway with *E. coli* for achieving higher product titers. This strategy might also be useful during the development of other microbial strains for the production of small metabolites of high value.

ACKNOWLEDGMENTS

This work was supported by the BOOST fund PNP-EXPRESS of the NRW Strategieprojekt BioSC and the Helmholtz Initiative Synthetic Biology of the Helmholtz Association.

We thank Petra Geilenkirchen (Forschungszentrum Jülich) for help with the LC-MS/MS analyses, Katharina Neufeld (University of Düsseldorf) for assisting with the chemical synthesis of *trans*-cinnamoyl-CoA, and Marco Bocola (RWTH Aachen University) for useful advice with the structural interpretation of the amino acid substitutions obtained in the HisPstrSTS2 variants.

REFERENCES

1. **Marienhagen J, Bott M.** 2013. Metabolic engineering of microorganisms for the synthesis of plant natural products. J Biotechnol **163:**166–178. http://dx.doi.org/10.1016/j.jbiotec.2012.06.001.
2. **Rivière C, Pawlus AD, Mérillon JM.** 2012. Natural stilbenoids: distribution in the plant kingdom and chemotaxonomic interest in Vitaceae. Nat Prod Rep **29:**1317–1333. http://dx.doi.org/10.1039/c2np20049j.
3. **Chong JL, Poutaraud A, Hugueney P.** 2009. Metabolism and roles of stilbenes in plants. Plant Sci **177:**143–155. http://dx.doi.org/10.1016/j.plantsci.2009.05.012.
4. **Park EJ, Chung HJ, Park HJ, Kim GD, Ahn YH, Lee SK.** 2013. Suppression of Src/ERK and GSK-3/beta-catenin signaling by pinosylvin inhibits the growth of human colorectal cancer cells. Food Chem Toxicol **55:**424–433. http://dx.doi.org/10.1016/j.fct.2013.01.007.
5. **Park EJ, Park HJ, Chung HJ, Shin Y, Min HY, Hong JY, Kang YJ, Ahn YH, Pyee JH, Lee SK.** 2012. Antimetastatic activity of pinosylvin, a natural stilbenoid, is associated with the suppression of matrix metalloproteinases. J Nutr Biochem **23:**946–952. http://dx.doi.org/10.1016/j.jnutbio.2011.04.021.
6. **Jeong E, Lee HR, Pyee J, Park H.** 2013. Pinosylvin induces cell survival, migration and anti-adhesiveness of endothelial cells via nitric oxide production. Phytother Res **27:**610–617. http://dx.doi.org/10.1002/ptr.4770.
7. **Jančinová V, Perečko T, Nosál R, Harmatha J, Šmidrkal J, Drábiková K.** 2012. The natural stilbenoid pinosylvin and activated neutrophils: effects on oxidative burst, protein kinase C, apoptosis and efficiency in adjuvant arthritis. Acta Pharmacol Sin **33:**1285–1292. http://dx.doi.org/10.1038/aps.2012.77.
8. **van Summeren-Wesenhagen PV, Marienhagen J.** 2013. Putting bugs to the blush: metabolic engineering for phenylpropanoid-derived products in microorganisms. Bioengineered **4:**355–362. http://dx.doi.org/10.4161/bioe.23885.
9. **Conde E, Fang WW, Hemming J, Willför S, Domínguez H, Parajó JC.** 2014. Recovery of bioactive compounds from *Pinus pinaster* wood by consecutive extraction stages. Wood Sci Technol **48:**311–323. http://dx.doi.org/10.1007/s00226-013-0604-1.
10. **Ferré-Filmon K, Delaude L, Demonceau A, Noels AF.** 2004. Catalytic methods for the synthesis of stilbenes with an emphasis on their phytoalexins. Coord Chem Rev **248:**2323–2336. http://dx.doi.org/10.1016/j.ccr.2004.02.011.
11. **Lim CG, Fowler ZL, Hueller T, Schaffer S, Koffas MAG.** 2011. High-yield resveratrol production in engineered *Escherichia coli*. Appl Environ Microbiol **77:**3451–3460. http://dx.doi.org/10.1128/AEM.02186-10.
12. **Watts KT, Lee PC, Schmidt-Dannert C.** 2006. Biosynthesis of plant-specific stilbene polyketides in metabolically engineered *Escherichia coli*. BMC Biotechnol **6:**22. http://dx.doi.org/10.1186/1472-6750-6-22.
13. **Donnez D, Jeandet P, Clément C, Courot E.** 2009. Bioproduction of resveratrol and stilbene derivatives by plant cells and microorganisms. Trends Biotechnol **27:**706–713. http://dx.doi.org/10.1016/j.tibtech.2009.09.005.
14. **Bhan N, Xu P, Khalidi O, Koffas MAG.** 2013. Redirecting carbon flux into malonyl-CoA to improve resveratrol titers: proof of concept for genetic interventions predicted by OptForce computational framework. Chem Eng Sci **103:**109–114. http://dx.doi.org/10.1016/j.ces.2012.10.009.
15. **Wu JJ, Liu PR, Fan YM, Bao H, Du GC, Zhou JW, Chen J.** 2013. Multivariate modular metabolic engineering of *Escherichia coli* to produce

resveratrol from L-tyrosine. J Biotechnol **167:**404–411. http://dx.doi.org/10.1016/j.jbiotec.2013.07.030.
16. **Park SR, Yoon JA, Paik JH, Park JW, Jung WS, Ban YH, Kim EJ, Yoo YJ, Han AR, Yoon YJ.** 2009. Engineering of plant-specific phenylpropanoids biosynthesis in *Streptomyces venezuelae*. J Biotechnol **141:**181–188. http://dx.doi.org/10.1016/j.jbiotec.2009.03.013.
17. **Katsuyama Y, Funa N, Miyahisa I, Horinouchi S.** 2007. Synthesis of unnatural flavonoids and stilbenes by exploiting the plant biosynthetic pathway in *Escherichia coli*. Chem Biol **14:**613–621. http://dx.doi.org/10.1016/j.chembiol.2007.05.004.
18. **Sambrook J, Russell D.** 2001. Molecular cloning: a laboratory manual, 3rd ed. Cold Spring Harbor Laboratory Press, Cold Spring Harbor, NY.
19. **Bauer JC, Wright DA, Braman JC, Geha RS.** August 1998. Circular site-directed mutagenesis. US patent 5,789,166A.
20. **Hanahan D.** 1983. Studies on transformation of *Escherichia coli* with plasmids. J Mol Biol **166:**557–580. http://dx.doi.org/10.1016/S0022-2836(83)80284-8.
21. **Marienhagen J, Kennerknecht N, Sahm H, Eggeling L.** 2005. Functional analysis of all aminotransferase proteins inferred from the genome sequence of *Corynebacterium glutamicum*. J Bacteriol **187:**7639–7646. http://dx.doi.org/10.1128/JB.187.22.7639-7646.2005.
22. **Marienhagen J, Eggeling L.** 2008. Metabolic function of *Corynebacterium glutamicum* aminotransferases AlaT and AvtA and impact on L-valine production. Appl Environ Microbiol **74:**7457–7462. http://dx.doi.org/10.1128/AEM.01025-08.
23. **Gross GG, Zenk MH.** 1974. Isolation and properties of hydroxycinnamate:CoA ligase from lignifying tissue of *Forsythia*. Eur J Biochem **42:**453–459. http://dx.doi.org/10.1111/j.1432-1033.1974.tb03359.x.
24. **Paczia N, Nilgen A, Lehmann T, Gätgens J, Wiechert W, Noack S.** 2012. Extensive exometabolome analysis reveals extended overflow metabolism in various microorganisms. Microb Cell Fact **11:**122. http://dx.doi.org/10.1186/1475-2859-11-122.
25. **Schomburg I, Chang A, Schomburg D.** 2014. Standardization in enzymology—data integration in the world's enzyme information system BRENDA. Perspect Sci **1:**15–23. http://dx.doi.org/10.1016/j.pisc.2014.02.002.
26. **Kodan A, Kuroda H, Sakai F.** 2002. A stilbene synthase from Japanese red pine (*Pinus densiflora*): implications for phytoalexin accumulation and down-regulation of flavonoid biosynthesis. Proc Natl Acad Sci U S A **99:**3335–3339. http://dx.doi.org/10.1073/pnas.042698899.
27. **Charpentier B, Bardey V, Robas N, Branlant C.** 1998. The EII^{Glc} protein is involved in glucose-mediated activation of *Escherichia coli gapA* and *gapB-pgk* transcription. J Bacteriol **180:**6476–6483.
28. **Moche M, Schneider G, Edwards P, Dehesh K, Lindqvist Y.** 1999. Structure of the complex between the antibiotic cerulenin and its target, beta-ketoacyl-acyl carrier protein synthase. J Biol Chem **274:**6031–6034. http://dx.doi.org/10.1074/jbc.274.10.6031.
29. **MacDonald MJ, D'Cunha GB.** 2007. A modern view of phenylalanine ammonia lyase. Biochem Cell Biol **85:**273–282. http://dx.doi.org/10.1139/O07-018.
30. **Röther D, Poppe L, Morlock G, Viergutz S, Rétey J.** 2002. An active site homology model of phenylalanine ammonia-lyase from *Petroselinum crispum*. Eur J Biochem **269:**3065–3075. http://dx.doi.org/10.1046/j.1432-1033.2002.02984.x.
31. **McKenna R, Nielsen DR.** 2011. Styrene biosynthesis from glucose by engineered *E. coli*. Metab Eng **13:**544–554. http://dx.doi.org/10.1016/j.ymben.2011.06.005.
32. **Cukovics D, Ehlting J, Van Ziffle JA, Douglas CJ.** 2001. Structure and evolution of 4-coumarate: coenzyme A ligase (4CL) gene families. Biol Chem **382:**645–654. http://dx.doi.org/10.1515/BC.2001.076.
33. **Kaneko M, Ohnishi Y, Horinouchi S.** 2003. Cinnamate: coenzyme A ligase from the filamentous bacterium *Streptomyces coelicolor* A3(2). J Bacteriol **185:**20–27. http://dx.doi.org/10.1128/JB.185.1.20-27.2003.
34. **Schneider K, Hövel K, Witzel K, Hamberger B, Schomburg D, Kombrink E, Stuible HP.** 2003. The substrate specificity-determining amino acid code of 4-coumarate:CoA ligase. Proc Natl Acad Sci U S A **100:**8601–8606. http://dx.doi.org/10.1073/pnas.1430550100.
35. **Schanz S, Schröder G, Schröder J.** 1992. Stilbene synthase from Scots pine (*Pinus sylvestris*). FEBS Lett **313:**71–74. http://dx.doi.org/10.1016/0014-5793(92)81187-Q.
36. **Raiber S, Schröder G, Schröder J.** 1995. Molecular and enzymatic characterization of 2 stilbene synthases from eastern white pine (*Pinus strobus*)—a single Arg/His difference determines the activity and the pH dependence of the enzymes. FEBS Lett **361:**299–302. http://dx.doi.org/10.1016/0014-5793(95)00199-J.
37. **Subrahmanyam S, Cronan JE.** 1998. Overproduction of a functional fatty acid biosynthetic enzyme blocks fatty acid synthesis in *Escherichia coli*. J Bacteriol **180:**4596–4602.
38. **Miyahisa I, Kaneko M, Funa N, Kawasaki H, Kojima H, Ohnishi Y, Horinouchi S.** 2005. Efficient production of (2S)-flavanones by *Escherichia coli* containing an artificial biosynthetic gene cluster. Appl Microbiol Biotechnol **68:**498–504. http://dx.doi.org/10.1007/s00253-005-1916-3.
39. **Zha WJ, Rubin-Pitel SB, Shao ZY, Zhao HM.** 2009. Improving cellular malonyl-CoA level in *Escherichia coli* via metabolic engineering. Metab Eng **11:**192–198. http://dx.doi.org/10.1016/j.ymben.2009.01.005.
40. **Leonard E, Lim KH, Saw PN, Koffas MAG.** 2007. Engineering central metabolic pathways for high-level flavonoid production in *Escherichia coli*. Appl Environ Microbiol **73:**3877–3886. http://dx.doi.org/10.1128/AEM.00200-07.
41. **Arnold K, Bordoli L, Kopp J, Schwede T.** 2006. The SWISS-MODEL workspace: a web-based environment for protein structure homology modelling. Bioinformatics **22:**195–201. http://dx.doi.org/10.1093/bioinformatics/bti770.
42. **Austin MB, Bowman ME, Ferrer JL, Schröder J, Noel JP.** 2004. An aldol switch discovered in stilbene synthases mediates cyclization specificity of type III polyketide synthases. Chem Biol **11:**1179–1194. http://dx.doi.org/10.1016/j.chembiol.2004.05.024.
43. **Ferrer JL, Jez JM, Bowman ME, Dixon RA, Noel JP.** 1999. Structure of chalcone synthase and the molecular basis of plant polyketide biosynthesis. Nat Struct Biol **6:**775–784. http://dx.doi.org/10.1038/11553.
44. **Shomura Y, Torayama I, Suh DY, Xiang T, Kita A, Sankawa U, Miki K.** 2005. Crystal structure of stilbene synthase from *Arachis hypogaea*. Proteins **60:**803–806. http://dx.doi.org/10.1002/prot.20584.
45. **Matsui T, Takita E, Sato T, Kinjo S, Aizawa M, Sugiura Y, Hamabata T, Sawada K, Kato K.** 2011. N-glycosylation at noncanonical Asn-X-Cys sequences in plant cells. Glycobiology **21:**994–999. http://dx.doi.org/10.1093/glycob/cwq198.
46. **Strasser R.** 2014. Biological significance of complex N-glycans in plants and their impact on plant physiology. Front Plant Sci **5:**363. http://dx.doi.org/10.3389/fpls.2014.00363.
47. **Chauhan JS, Rao A, Raghava GPS.** 2013. *In silico* platform for prediction of N-, O- and C-glycosites in eukaryotic protein sequences. PLoS One **8:**e67008. http://dx.doi.org/10.1371/journal.pone.0067008.
48. **Xu P, Ranganathan S, Fowler ZL, Maranas CD, Koffas MAG.** 2011. Genome-scale metabolic network modeling results in minimal interventions that cooperatively force carbon flux towards malonyl-CoA. Metab Eng **13:**578–587. http://dx.doi.org/10.1016/j.ymben.2011.06.008.